CHINA SHIP SCIENTIFIC RESEARCH CENTER

Laser Velocimeter Measurements and Cavitation Observation on Two Axisymmetric Bodies

Ye Yuan-Pei Wang Dao-Zheng

April 1986

CSSRC Report
English version-86003

P . O . BOX 116, WUXI, JIANGSU

CHINA

Contents

ABSTRACT

Recent flow measurements on a longitudinal blunt circular cylinder and a 1.5 cal ogive with a groove using a two dimensional direction-sensitive laser velocimeter are reported in the present paper. The tests were performed in a water tunnel with a test section of $600 \times 600 mm^2$. Tested Reynolds number ranged from 0.75×10^5 to 6×10^5. Profiles of the axial and radial mean velocity components and RMS values of the two fluctuating components were obtained. Spectrum analysis of the RMS signals was performed. It has been found that when transition occurs the velocity level is increasing linearly with decreasing of the frequency in a log-log plot on the power spectrum. In this case the ratio of low pass filtered RMSvalue to high pass filtered onereaches a maximum. Cavitation observations confirmed that inception often occured in the neighbourhood of the low-pressure centers of vortex cores ($\bar{u}$ =0) both in shear layer of the blunt circular cylinder and in groove of the 1.5 cal ogive.

NOMENCLATURE

C_p	pressure coefficient = $(p-p_\infty)/\frac{1}{2}\rho\bar{U}_\infty^2$
D	maximum diameter of the cylinder
h	radial distance from the body surface
L	reattachment length
LDV	Laser Doppler Velocimeter
p	local static pressure
p_v	vapour pressure at ambient temperature
p_∞	free stream static pressure
R_{eD}	Reynolds number = $U_\infty D/\nu$
RMS	root mean square
u	axial component of velocity
U_e	velocity at boundary layer thickness
U_∞	free stream velocity
v	radial component of velocity
x	axial distance from the stagnation point
Γ	circulation
Δh	groove dimension
ν	kinematic viscosity of water
ρ	dinsity of water
σ	cavitation index = $(p_\infty-p_v)/\frac{1}{2}\rho U_\infty^2$
i	incipient
d	desinent
-	average value
'	fluctuating value

1. INTRODUCTION

There have been numerous studies on flow and cavitation in large separated region since the early work by Kermeen and Parkin [1]. They investigated cavitation benind sharp edge disks. They found that inception occured only in the shear layer and cavitation index increased considerably with increase of the body Reynolds number. They used a model of cavitation occuring at the low-pressure centers of vortex cores to predict inception. Later Arndt reanalyzed their data and proposed a semiempirical approach assuming that the near wake could be idealized by an axisymmetric shear layer containing discrete ring vort ces

of strength Γ {2}, Katz studied the cavitating flow around blunt circular cylinder {3,4}. He used holography for flow visualization and cavitation observation. He compared his data of location of cavitation inception with the hot-wire anemometer results by Ota and Ota and Motegi {5,6}. He also measured surface pressure fluctuation, however these pressure peaks did not display any difinite dependence on the Reynolds number to explain the inception phenomenon occured far from the body surface. Recently, Katz and O'Hern studied cavitation phenomenon in the shear layer behind a two-dimensional sharp-edge plate {7}. They found that cavitation inception occured in the "secondary" axial vortices of the mixing layer between the spanwise coherent eddies. Their inception data displayed a strong dependence on the air content. On the other hand, Arakeri et al investigated cavitation inside a groove on a 1.5 cal ogive to study whether rectified diffusion could be an important mode of bubble growth in separated regions {8}. They used Schlieren method to determine boundary layer transition and measured surface pressure fluctuation at the groove bottom.

Although much progress has been achieved in the past, in order to get a better understanding of the close relation between the turbulent flow field and cavitation phenomena around bodies with large separation regions, more detailed and accurate information about the back flow region is still needed. This is our first attempt to use LDV as a quantitative flow visualization measure of an extensive program to study cavitation scale effect. Our preliminary objective of the present study is limited to use LDV to determine the separation, transition and reattachment point and to obtain flow characteristics in the back flow region of the blunt circular cylinder and inside the groove on the 1.5 cal ogive.

2. EXPERIMENTAL PROCEDURES

A longitudinal blunt circular cylinder and a 1.5 cal ogive with a square groove were tested. The maximum diameter of the cylindrical afterbody of these two models is 64mm. The models were mounted directly on the axis of the water tunnel with a test section of 600 × 600mm^2. The diameter of the axis is approximately the same as the two models. A LDV type 9109 made by TSI was used. Mean and RMS values of axial and radial velocity were obtained together with the RMS signal recorded by tape recorder either B & K 7003 ($f < 20KH_z$) or TEAC R81 ($f < 5KH_z$). Real time analysis was also made with a B & K Heterodyne Analyzer 2010 and a level recorder B & K 2307. Cavitation observation was made under stroboscopic light. Typical conditions were recorded on video tape, photos and slides were also taken. The inception and desinence measurements were made in the routine manner. In case the difference between these two measurements is not significant, only the average value of cavitation index σ is used.

3. RESULTS AND DISCUSSION - BLUNT CIRCULAR CYLINDER

3.1 LDV Measurements

Ota and Ota and Motegi used a constant temperature hot-wire anemometer with linearizer to measure the flow around a longitudinal blunt circular cylinder in a low speed wind tunnel. Many singificant results about the separated flow region were obtained, such as the reattachment length, the maximum reverse velocity and maximum value of turbulent ve-

locity, etc. Their main conclusion was that the flow characteristics were indepedent of Reynolds number. However, from a view point of cavitation research their information seems not enough. Firstly, both the Reynolds number itself and its range in their test were not large enough. Secondly, hot-wire anemometer is difficult to be used in such a separated flow region with large turbulence intensity. As can be seen from their results that no data of radial turbulent fluctuating velocity is available in the inner half region of interest, and it is this component of velocity fluctuation that should be correlated with pressure fluctuation in the boundary layer {9} . Ota and Motegi estimated that the uncertainty of nondimensional turbulence intensity might be higher than ±30 percent in this region. It is generally accepted that these uncertainties may become less by using LDV. Based on these considerations our measurements were performed. Fortunately, our LDV results have turned out to be basically the same as Ota and Ota and Motegi's. So it is not necessary to present all the detailed results here. The major difference between the present LDV results and theirs is that the flow characteristics such as reattachment length, mean velocity and RMS values of fluctuating velocity are still dependent of Reynolds number in the tested range of Reynolds number from 0.75×10^5 to 6×10^5, although this dependence is not strong. From Fig. 1 it can be seen that the reattachment length is decreasing with the increasing Reynolds number. The maximum reverse velocity and turbulence intensity also display the same trend. For example, when R_{eD} equals 2×10^5, $L/D\doteq1.6$, $|-\bar{u}|_{max}=0.4$ and $\sqrt{\overline{u'^2}}=0.3$, when R_{eD} equals 4×10^5, $L/D\doteq1.5$, $|-\bar{u}|_{max}=0.3$ and $\sqrt{\overline{u'^2}}=0.2$. Another difference is that in our case $\sqrt{\overline{v'^2}}$ can be measured in the whole separated region, it does not show such large scatter as appeared in the previous measurement. It has been found that no sharp maxima of $\sqrt{\overline{u'^2}}$ and $\sqrt{\overline{v'^2}}$ appear inside the downstream part of the separated region and there is no significant difference between the RMS values of fluctuating velocity at locations where $\sqrt{\overline{u'^2}}$ = max and $\bar{u}=0$, Fig.2.

3.2 Cavitation Observation

Fig.3 shows two sets of cavitation indices averaged from inception and desinence measurements corresponding to lower and higher free air content respectively. The lower results indicate that σ increases from 1.35 to 1.52 when R_{eD} increases from 2.38×10^5 to 5.55×10^5. These results are in good agreement with Kermeen and Parkin's result behind sharp-edge disks and Katz's result on a two inch blunt body. Another set of data on the same figure corresponds to a higher free air content case resulted from leakage of air into the tunnel. Cavitation index increase linearly with decreasing of Reynolds number, as is well known that it represents a typical tendency of gaseous cavitation. Fig.4 is a drawing of the first traces of inception cavitation accumulated from 36 slides taken at the same condition, $R_{eD}=4\times10^5$ and $\sigma=\sigma_i\doteq2.0$. Two lines corresponding to $\bar{u}=0$ and $\sqrt{\overline{u'^2}}$ = max are also shown on the same figure. It is obvious that onset of cavitation inception occured between these two lines. From the measurement results by Ota and Katz, the minimum pressure locates at the point of $X/D\doteq0.7$ with a value of Cp_{min} of -0.6. Our LDV result indicates that the maximum turbulence intensity of 0.3 exists in the above mentioned shear layer which may cause a maximum pressure fluctuation of $\Delta Cp\doteq0.1$. Therefore it is impossible to attribute the high cavitation index of 1.5 to velocity or pressure fluctuation only. It seems probable that in the neighbourhood of the low-pressure centers of

vortex cores there is more than enough time for gaseous cavitation to grow. As indicated by Ye, the tendency of increase of cavitation index with increasing speed appeared both in the higher speed range of vortex flow and for the flow with separation bubble may also indicate a gas content effect {10} .

3.3 Spectrum Analysis

The recorded RMS signal was first analyzed using a B & K High Resolution Signal Analyzer Type 2033 in the frequency range of 0-100 Hz, 0-500 Hz and 0-10KHz. The analysis indicates that there appears no sharp peak or characteristic frequency on the power spectrum of turbulent velocity. Only a broad hump near 7 KHz has been found for the lowest Reynolds number. When R_{eD} increases this hump disappears. This hump is thought to be produced by the Tollmien-Schlichting wave in the boundary layer. Because the peak RMS value is of primary importance to correlate velocity fluctuation data with cavitation, a kind of so called "hold-max spectrum" was also obtained to compare with the usual power spectrum. It was found that the difference between the average RMS and peak RMS values was 6-7 dB for $R_{eD}=0.75\times10^5$ and nearly 10 dB for Red $\doteq 4\times10^5$ in the whole frequency range of 10KHz.

4. RESULTS AND DISCUSSION - 1.5 CAL OGIVE

4.1 Test Model

An axisymmetrical square groove of $1.28\times1.28mm^2$ was cut on a 1.5 cal ogive at X/D=1.30. This groove location was chosen based on the previous similar study by Arakeri et al and Arakeri {11}. It was estimated that in the present tested range of Reynolds number boundary layer transition would occur above this groove location.

4.2 LDV Measurements

Profiles of the axial and radial mean velocity components and RMS values of the two fluctuating components of velocity were obtained including distribution inside the groove, Figs. 5-8. A comparison of these profiles with typical well-known boundary layers such as Blasius profile and 1/7th power profile was made. Different types of laminar, transitional and turbulent boundary layers do appear in the present test. Distributions inside the boundary layer above the groove including distribution down to the groove bottom are given on Figs. 7 and 8. Obviously, a vortex ring with $\bar{u}=0$ at the groove center is formed around the cylinder. In spite of the different flow regime velocity fluctuation always exists inside the groove. So the velocity field inside the groove appears always unsteady.

4.3 Cavitation Observation

Fig.9 shows two sets of cavitation indices, the lower one is the average value from inception and desinence measurements corresponding to a lower free air content and the higher one includes separate incep - tion and desinent cavitation indices corresponding to a higher free air content resulted from the leakage of air into the tunnel. Careful observation of the cavitation inception phenomenon in the groove was made both visually and by recording on video tape under stroboscopic and ordinary light. With cavitation inception few bubbles of size

0.3-0.4mm were found along the groove. As first reported by Arakeri et al these bubble then would move around circumferentially within the groove. They may either move very fast appearing as suddenly falling down from the top of the cylinder. Or osillate near some fixed location for a quite long period of time. Both clockwise and counter-clockwise rotation were found. When the flow was full of cavitation nuclei even the gradual growth process of the bubble inside the groove could be observed as it was falling down from the top of the cylinder. Fig.10 is a typical shadowgraph, from which the most probable location of cavitation inception has been found almost at the center of the groove. The bubble inside the groove is often detached away from the groove bottom, only once in a while it moves down to the bottom but does not stay there.

Based on the surface pressure fluctuation measurements by Arakeri et al and our cavitation indices obtained with higher free air content, it seems no doubt that groove cavitation is a type of gaseous cavitation. It is interesting to note that in the present test, cavitation also occured even when the boundary layer above the groove is laminar.

4.4 Spectrum Analysis and Detection of Transition

The recorded RMS signal was analyzed using a B & K Heterodyne Analyzer type 2010 in the frequency range of 2Hz-2kHz and 20Hz - 20kHz Figs. 11-13 are power spectrums of axial fluctuating velocity at tangency point of X/D = 1.11 for $R_{eD1} = 1.64\times10^5$, $R_{eD2} = 3.84\times10^5$, $R_{eD3} = 6.07\times10^5$. For $R_{eD} = R_{eD2}$ the radial distribution of axial velocity looks very much like the laminar Blasius profile. For $R_e = R_{e3}$, it looks like the turbulent 1/7th power distribution. For $R_e = R_{e1}$, a second peak appears at higher frequency which is thought to be caused by the Tollmien-Schlichting wave. It can be seen from these spectrums that with the development of transition process intensity level becomes higher at low frequency range, especially when transition occurs the velocity level is increasing linearly with decreasing of the frequency in a log-log plot on the power spectrum. In this case the ratio of low pass filtered RMS value to higher pass filtered one reaches a maximum {12}. The ratio of RMS value obtained with different band pass filter of 0-1 KHz and 1 KHz - 20 KHz is given in Table 1. When transition occurs this ratio is greater than 4. Thus transition of boundary layer can be detected using a LDV either by comparison of RMS values with different band pass filter or by spectrum analysis according to the above mentioned two criteria, namely a maximum ratio of RMS values greater than 4 or a linear increase of intensity level with de rease of frequency in a log-log plot of power spectrum.

Table 1. Comparison of Ratio of RMS Values of Axial Fluctuating Velocity Using Different Band Pass Filters

Axial Distance X/D	Radial Distance h mm	$R_{eD} \times 10^5$ 1.64	3.84	6.07
1.11	0.18	1.71	2.87	4.84
1.30	0.18	3.42	5.22	3.55
1.31	0.18	3.34	4.80	
1.31	-0.02		3.58	4.15
1.31	-1.22		2.88	3.58
1.32	0.18	3.36	4.02	3.31
2.00	0.18	3.34	2.49	6.90

5. CONCLUDING REMARKS

The significant results of the present study can be summarized as follows:

1. Flow characteristics were measured by LDV with more accuracy than the previous hot-wire anemometer measurement. Such characteristics as reattachment length, mean velocity and RMS value of fluctuating velocity are found to be still dependent of Reynolds number in the range of $0.75\times10^5 < R_{eD} < 6\times10^5$.

2. LDV can be used to detect boundary layer transition. Spectrum analysis of the RMS values of fluctuating velocity indicates that when transition occurs the velocity level is increasing linearly with decreasing of the frequency in a log-log plot on the power spectrum. In this case the ratio of low pass filtered RMS value to high pass filtered one reaches a maximum. Transition detection on a 1.5 cal ogive by this method shows good agreement with the result of Schlielen method, Fig.14.

3. Detailed information about the flow inside a small groove is given by the present LDV measurement. Different flow patterns of the boundary layer above the groove such as laminar, transitional and turbulent do not strongly effect the flow field inside the groove. Groove cavitation also occurs when the above boundary layer is laminar.

4. Groove cavitation bubble locates near the center of ring vortex core inside the groove. However maxima of both RMS values of fluctuating velocity are at the top of the groove, and these maxima equal to 2-5 times the RMS values at the center. This fact alone suggests that the long residence time is more important for cavitation inception than the pressure or velocity fluctuation.

5. Cavitation inception around the blunt circular cylinder is found to be concentrated in the neighbourhood of the low-pressure centers of ring vortex cores.

6. When there exists a large amount of nuclei, a well-known typical tendency of gaseous cavitation appears for both models, namely cavitation index increases with decrease of Reynolds number. Because the opposite tendency of increase of cavitation index with increase of Reynolds number may also indicate a gas content effect, it seems reasonable to explain the high cavitation index as caused by gaseous cavitation instead of by pressure fluctuation alone.

ACKNOWLEDGEMENT

This work is sponsored by the Science Foundation of the Chinese Academy of Sciences.

REFERENCES

1. Kermeen, R.W., Parkin, B.R., "Incipient Cavitation and wake Flow Behind Sharp Edge Disks", California Institute of Technology, Hydrodynamic Lab., Report No. 85-4 August, 1957.

2. Arndt, R.E.A., "Semiempirical Analysis of Cavitation in the Wake of a Sharp Edged Disk", J. Fluid Engineering, Vol.98, 1976, pp. 560-562.

3. Katz, J., "Cavitation on a Body with a Large Separation Region", ASME Cavitation & Polyphase Flow Forum, 1982.

4. Katz, J., "Cavitation Inception in Separated Flows", Ph.D. Thesis, Calif. Inst. of Tech., Report No. 183-5, 1981.

5. Ota, T., "An Axisymmetric Separated and Reattached Flow on a Longitudinal Blunt Circular Cylinder", Trans. ASME, J. of Applied Mechanics, Vol. 42, 1975, pp.311-315.

6. Ota, T., Motegi, H., "Turbulence Measurements in an Axisymmetric Separated and Reattached Flow over a Longitudinal Blunt Circular Cylinder", J. of Applied Mechanics, Vol. 47, March, 1980, pp.1-6

7. Katz, J., O'Hern, T.J., "Cavitation in Large Scale Shear Flows", ASME paper 83-FE-33, 1983.

8. Arakeri, V.H., Milton, S.G., Sharma, S.D., "Role of Unsteady Pressure Fields in Cavitation Inception", Proc. Int. Symp. Cavitation Inception - 1984, pp.69-74.

9. Arndt, R.E.A., "Recent Advances in Cavitation Research", Advances in Hydroscience, Vol.12, 1981.

10. Ye, Y.P., "Some Aspects of Hub Vortex Cavitation", Proc. Int. Symp. Cavitation Inception - 1984, pp.177-189.

11. Arakeri, V.H., "A Note on the Transition Observations on an Axisymmetric Body and Some Related Fluctuating Wall Pressure Measurements", Trans. ASME J. of Fluids Engineering, Vol.97, Series 1, No.1, March, 1975, pp.82-87.

12. Lauchle, G.C., "Noise Generated by Axisymmetric Turbulent Boundary-Layer Flow", J. Acoust. Soc. Am. Vol. 61, No.3, March 1977, pp. 694-703.

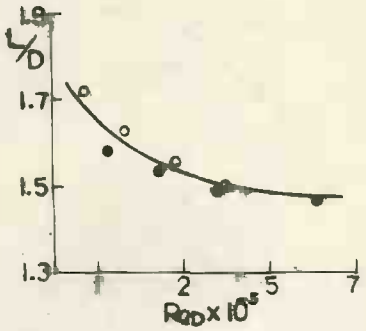

Fig. 1 The reattachment length on the blunt circular cylinder

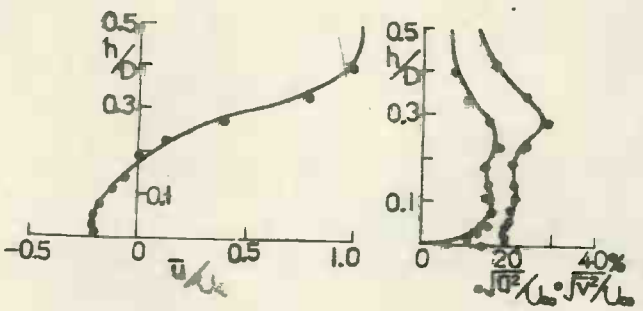

Fig. 2 Mean axial velocity Turbulence intensity
X/D = 0.917,
$R_{eD} = 6 \times 10^5$

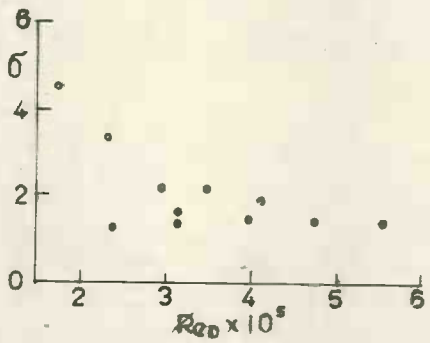

Fig. 3 Cavitation indices on the blunt circular cylinder

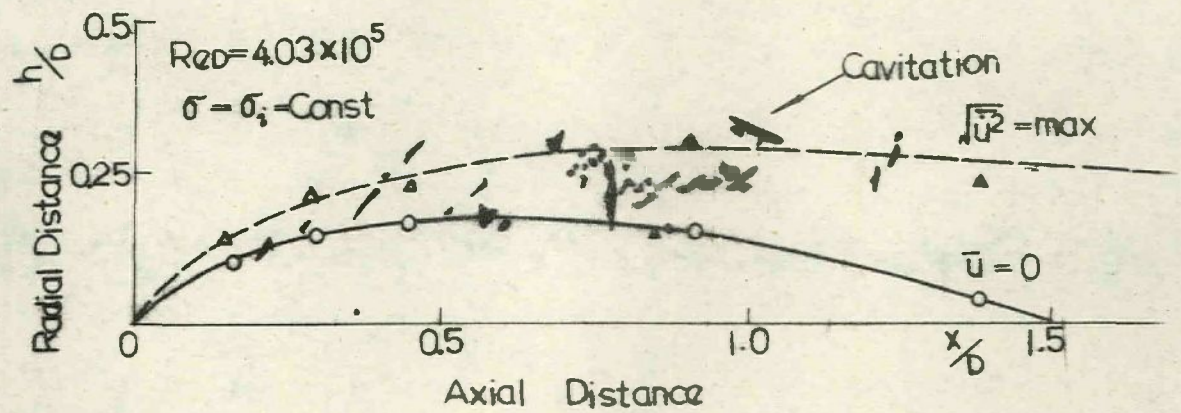

Fig. 4 The first cavitation traces within the flow field on the blunt body

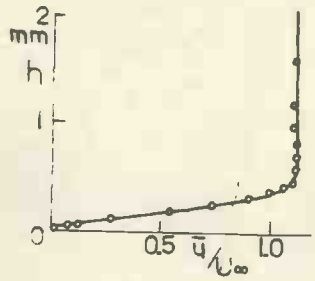

Fig. 5 Mean axial velocity

$R_{eD} = 3.84 \times 10^5$,

X/D = 1.11

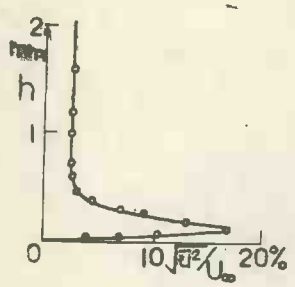

Axial turbulence intensity

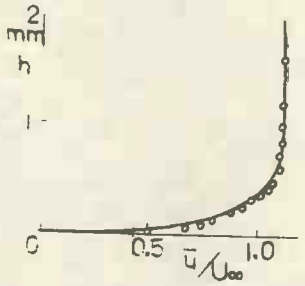

Fig. 6 Mean axial velocity

$R_{eD} = 6.07 \times 10^5$,

X/D = 1.11

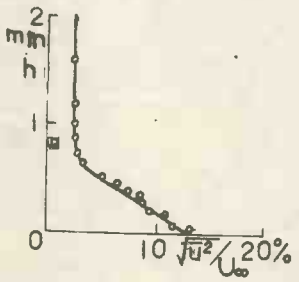

Axial turbulence intensity

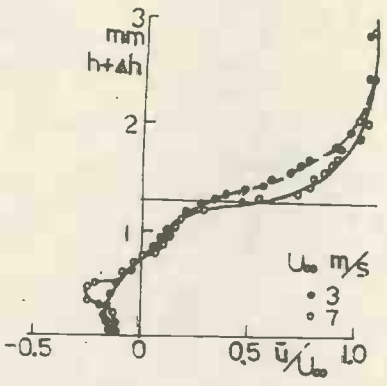

Fig. 7a Mean axial velocity,

X/D = 1.31

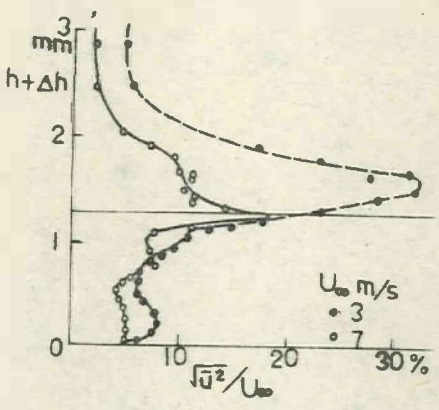

Fig. 7b Axial turbulence intensity X/D = 1.31

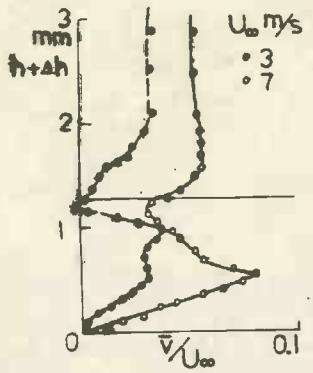

Fig. 8 Mean radial velocity, X/D = 1.31

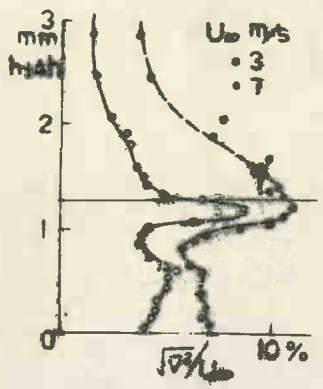

Radial turbulence intensity

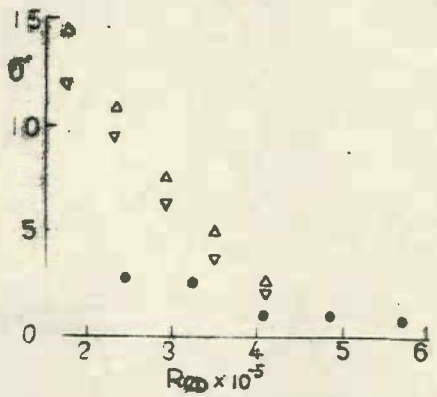

Fig. 9 Cavitation indices on the 1.5 cal ogive

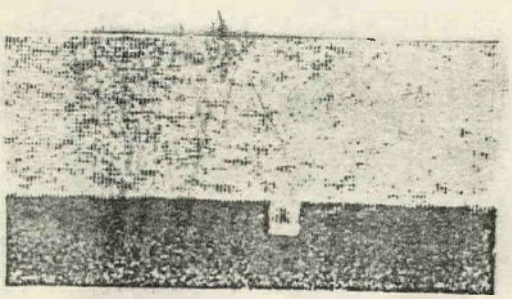

Fig. 10 Shadowgraph of groove cavitation

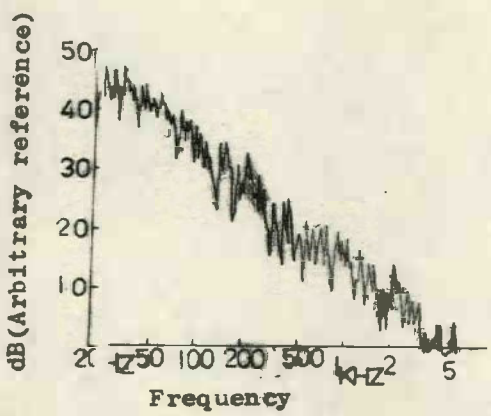

Fig. 11 Axial turbulence intensity $R_{eD} = 6.07 \times 10^5$, X/D = 1.11

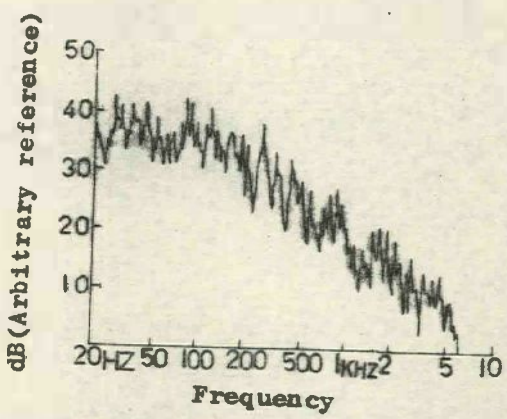

Fig. 12 Power spectrum of axial turbulence intensity, $R_{eD} = 3.84 \times 10^5$, X/D = 1.11

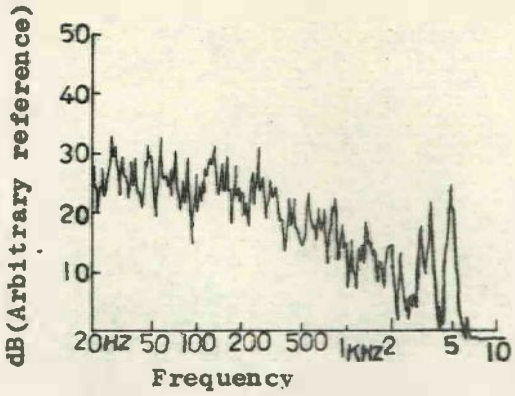

Fig. 13 Axial turbulence intensity

$R_{eD} = 1.64 \times 10^5$, X/D = 1.11

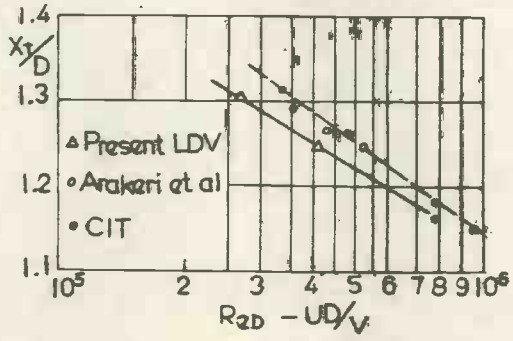

Fig. 14 Comparison of transition location on the 1.5 cal ogive by different detection methods